IJIE

http://penerbit.uthm.edu.my/ojs/index.php/ijie
ISSN : 2229-838X e-ISSN : 2600-7916

The International Journal of Integrated Engineering

Performance of Photogrammetry-Based Makeshift 3D Scanning System for Geometrical Object in Reverse Engineering

Muhammad Nur Farhan Saniman[1*], Hariz Syahmi Zulkifli[1], Muhammad Izhar Ishak[2], Khairul Anuar Abd Wahid[1], Amzari Zhahir[3], Wan Mansor Wan Muhamad[1]

[1]Mechanical Engineering Section,
Universiti Kuala Lumpur Malaysia France Institute, Bandar Baru Bangi, 43650, MALAYSIA

[2]Department of Mechanical Engineering, College of Engineering,
Universiti Malaysia Pahang, Pekan, 26600, MALAYSIA

[3]Department of Aerospace Engineering, Faculty of Engineering,
Universiti Putra Malaysia, Serdang, 43400, MALAYSIA

*Corresponding Author

DOI: https://doi.org/10.30880/ijie.2023.15.07.005
Received 6 September 2022; Accepted 3 October 2023; Available online 5 December 2023

Abstract: A three-dimension (3D) scanner is one of the important tools for digital reproduction of physical objects in reverse engineering. In some cases, a makeshift 3D scanner is needed immediately, such as for emergency spare parts reproduction. Thus, this research aims to investigate the feasibility of a low-cost makeshift 3D scanner using a mobile phone and the photogrammetry method in reconstructing digital 3D models of geometrical objects. A focus is given to the dimension accuracy of the reconstructed 3D models, which have been reproduced using images taken by a mobile phone, in comparison with the actual dimension of the scanned test pieces. To do so, four types of actual geometrical test pieces with dimension from 5 mm to 175 mm were fabricated using a CNC machine. 3D models of each test pieces had been developed using the photogrammetry method and compared with those developed using an industrial-grade high-end 3D scanner. It was found that mobile photogrammetry achieved an average accuracy of 97.2%, with minimum and maximum values of 83.3% and 99.9%, respectively. Geometrical dimensions less than 10 mm tend to have lower accuracy, while it was the opposite for dimensions over 150 mm. Furthermore, the scanning limit for either method was found to be a surface with a small tilting angle (less than 3 degrees). Nevertheless, photogrammetry method in combination with a mobile phone has the potential to be utilized as an alternative of a makeshift 3D scanning system with sufficient accuracy using commonly available tools.

Keywords: 3D scanning, makeshift, geometrical accuracy, photogrammetry, reverse engineering

1. Introduction

Reverse engineering involves the process of digital reconstruction of actual object into computer aided design 3D model is one of the necessities for related key players, especially in the field of mechanical and biomedical industries. An example of such a situation is when a crucial component for a machine is faulty and no spare part is immediately

*Corresponding author: mnfarhan@unikl.edu.my

available. The presence of 3D models will not only be useful in reproducing the spare part, but also will help engineers to conduct computer analysis for design improvement. Since rebuilding complicated shapes and surfaces are very time consuming and expensive, instead of using contact methods such as analogue coordinate measuring machine (CMM) [1], engineers rely on more versatile alternative of non-contact approach by using 3D scanning devices to reconstruct 3D models [2]. As a result, the utilization of 3D scanning systems in various industries has increased by more than ten times in the past ten years [3].

Although 3D scanning devices can be very helpful for designers or engineers, the current market price for industrial-grade 3D scanners is ranging from approximately USD 10,000 to 50,000 [4], or even more. Such prices are only affordable for large enterprises or specific professionals, thus, many small and medium industries, as well as individuals, are opting for much cheaper alternatives. Moreover, in most cases, they often do not need all the features of a full reverse engineering package. Instead, such non-experts are more concerned with the ease-of-use, cost-effective, and time-saving solutions that could deliver the intended results [5]. Therefore, due to the urges and needs for a low-cost yet sufficiently reliable 3D scanning system, alternative technologies have been developed.

Among available alternative technologies, a laser line scanner has been used for inspecting parts in the production line [6]. Despite having moderate accuracy with a low-cost system, automated line scanning can be achieved. Moreover, depth cameras also have been used for 3D sensing, which typically uses time-of-flight [7] or structured light [8] principle. Examples of such depth cameras are Microsoft Kinect [9] and Google Tango [10]. Other than that, low-cost 3D scanning systems also have been developed using a digital single-lens reflex (DSLR) camera [2] and web camera [11]. Photogrammetry has been used for the same purpose. However, until recently, it is noted that the digital photogrammetry approach has been consistently and rapidly developed with many proposed novel measurement principles [12].

In close-range digital photogrammetry, the 3D digital models are created based on overlapping stereoscopic images that produced dense point clouds to provide geometric information. A sufficient number of images from different perspectives with 60-80% overlapping is needed to reconstruct the 3D model using specialized software. The higher the number of source images, the lower the possibility of modeling error due to blind zones. It is also important to have clear and sharp images to develop an accurate 3D model [13]. Among the advantages of using photogrammetry are realistic digital models, increased accuracy, reduced equipment cost, and increased throughput [14].

Aside from the economical factor, the accuracy of a 3D scanning system to comply with existing physical scanned objects plays a significant value. Even though digital photogrammetry has been applied in various fields such as archeology [15], biology [16], topography [17] and geology [18], only several examples could be found on engineering application, especially for geometrical objects, such as Pelton bucket and turbine blade runner [19]. It could be due to the uncertainty on the accuracy of such method [20]. Thus, it is important to investigate the feasibility and reliability of the makeshift 3D scanning method based on the photogrammetry technique.

This study aims to investigate the accuracy of a low-cost makeshift 3D scanning system based on photogrammetry method using a mobile phone to capture images of various geometrical test pieces. Using the captured images, reconstructed 3D models by mobile photogrammetry will be compared to that of 3D models reconstructed using an industrial-grade high-end scanner. The accuracy, as well as measurement error, will be presented, and the feasibility of such method for reverse engineering will be discussed.

2. Methodology

2.1 3D Modelling of Geometrical Objects

In order to evaluate the feasibility and performance of photogrammetry-based mobile 3D scanning system, the process begins with designing the test piece. Four 3D models (label X, Y, G, and H) comprising of various combinations of various geometrical shapes such as rectangular, triangle, and circle, as well as straight and curvy lines, were designed using Solidworks software. Details of the design are shown in Fig. 1 and the dimension value for each label are given in Table 1. The thickness for all models was 20 mm.

2.2 Fabrication of Test Pieces

The test pieces then were fabricated using three axes Computer Numerical Control (CNC) milling machine (KAFO CVM-9B) according to the dimensions of designed 3D models. A high-density polyethylene (HDPE) material (density 930~970 kg/m^3) was chosen as the material due to its recyclability and large strength to density ratio that can withstand the machining heat without deformation.

2.3 Dimension Measurement

The dimensions of the fabricated test pieces as shown in Figure 1 were measured using digital Vernier caliper and protractor with accuracy of 0.01 mm and 0.1°, respectively. For test piece X, Y, G, and H, there were 16, 9, 15, and 8 measured dimensions, respectively, as shown in Table 1. For each dimension, 6 repetitive measurements were conducted, and the average values were used in the discussion.

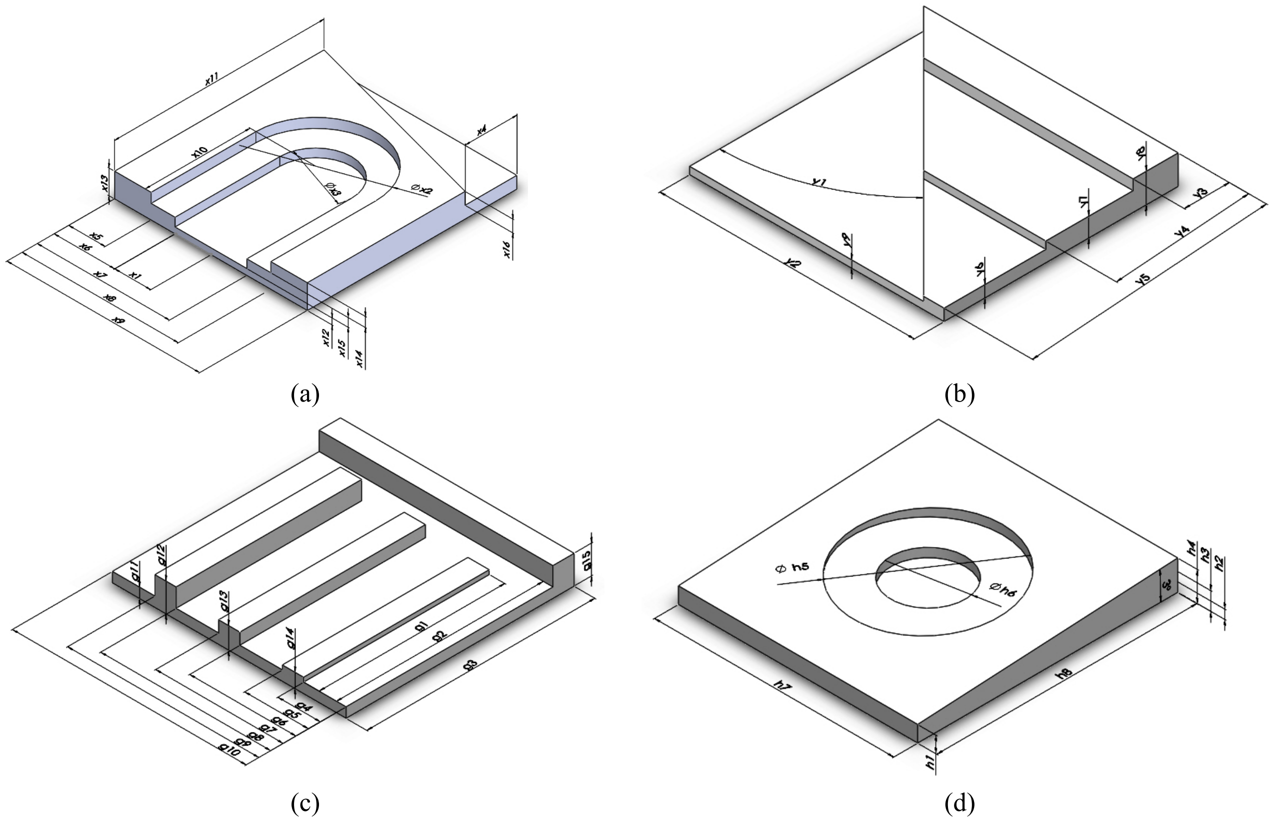

Fig. 1 - Isometric view for test piece (a) *X*; (b) *Y*; (c) *G*, and; (d) *H*

2.4 3D Scanning Methods

Two different 3D scanning methods have been utilized in this study in order to quantitatively analyze the performance of both 3D scanners.

2.4.1 Mobile Photogrammetry

The Photogrammetry method involves taking a lot of images of the test piece, which then will be combined to construct the corresponding 3D model. In this study, a mobile phone (Apple iPhone 10) has been used to take pictures of the test pieces from various angles. Any mobile phone could be used for such purposes, as long as it has a phase detection autofocus (PDAF) function to assist in capturing high-quality sharp images. The test piece is set on a flat surface. Mobile phones are positioned vertically at a constant distance of 1 m from the center of the test piece. By maintaining the distance and setting the center of the test piece as a fix point, the camera is rotated upward at 30^o angle. Then, a series of photographs are taken for one complete rotation with the interval of 18^o to the right, with a total of 20 images. These steps are repeated by rotating the mobile phone upward at 50^o, as shown in Fig. 2. Then, those images were combined using Meshroom, a free non-commercial prominent software for photogrammetry. The constructed 3D meshes in Meshroom were exported in an .OBJ file format, which later were trimmed and converted to .STL file format using Meshmixer software, so that the reconstructed 3D models could be opened in Solidworks for dimension accuracy evaluation.

2.4.2 High-end Industrial Grade 3D Scanner

For comparison purposes, a professional high-end industrial-grade 3D scanner (Creaform Go! SCAN50) together with accompanied software (Creaform VXelement) has been used to scan, capture images, and reconstruct the 3D models of all four test pieces. The device has a maximum of 0.5 mm resolution with an acquisition speed of 550000 points/s. The optimum scanning range is approximately 0.4~0.65 meters from the test pieces, where no specific positioning angle is required. A high accuracy of reconstructed 3D models is expected owing to its optical triangulation technique in determining the dimension of the scanned objects. Despite such high specifications, an experienced user is necessary to obtain good, reconstructed 3D models. The 3D models then were exported in .STL file format to be used in Solidworks software.

2.5 Performance Analysis

In order to determine the performance and reliability of the makeshift photogrammetric based 3D scanning system, the percentage accuracy, a, of reconstructed 3D models was calculated by:

$$a = \left(1 - \frac{\left|V_{observed} - V_{true}\right|}{V_{true}}\right) \times 100 \quad (1)$$

Here, V_{true} and $V_{observed}$ are the original dimension of fabricated test pieces and measured dimension of reconstructed 3D models, respectively, either by mobile photogrammetry or high-end scanner. Furthermore, using a statistical method of two-factors analysis of variance (ANOVA), the performance of mobile photogrammetry will be evaluated quantitatively and the suitability of such system for the mechanical industry will be discussed. Such a statistical method was chosen since it could provide a comprehensive understanding about the interaction and significance between the mobile photogrammetry and high-end scanner for 3D scanning in reverse engineering.

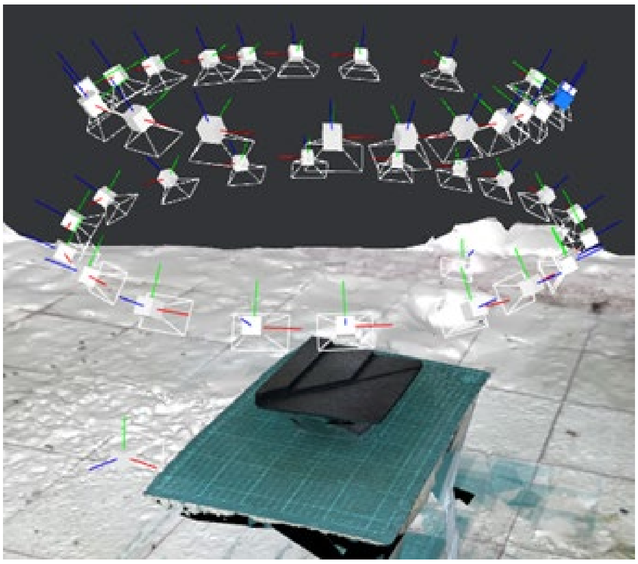

Fig. 2 - Final 3D reconstruction of part Y and its position and orientation of camera

3. Results and Discussion

Fig. 3 shows the reconstructed 3D models by mobile photogrammetry and high-end 3D scanner. Such figures indicate that the 3D scanning system via mobile photogrammetry managed to produce similar 3D models of the test pieces as of the high cost high-end 3D scanner. It could be observed in Figs. 3(e) to 3(l) that the reconstructed surface textures by both techniques are comparably smooth. However, detailed inspection on the reconstructed models revealed that the high-end scanner was able to produce smoother edges. Even though such qualitative deduction based on visual inspection on the reconstructive 3D models does not absolutely reflect the actual performance of mobile photogrammetry, it has become apparent that even without a high-end 3D scanner, a satisfactory reverse engineering is feasible by merely using basic equipment such as a mobile phone's camera and a personal computer.

In order to quantitatively evaluate the performance of the mobile photogrammetry, the measured dimensions of reconstructed 3D models by both 3D scanning methods, mobile photogrammetry and high-end scanner, are tabulated in Table 1. The dimension differences for both methods in comparison with the fabricated dimension are also included. Positive difference means the reconstructed dimension is larger, and vice versa. By comparing the magnitude of difference between both methods, it could be observed that those of mobile photogrammetry are larger. These large magnitudes of difference indicate a lower capability of photogrammetry method in producing the reconstructed geometry 3D model with high accuracy. Since photogrammetry-based 3D scanning relies based on the images taken, there are a lot of factors that could affect the quality of the 3D model. Light reflection and point focus could affect the texture, which is also mentioned in previous study [21], while the number of photo redundancy (number of pictures for a full rotation) and point angle (number of angles to take the pictures) could affect the sharpness of the reconstructed model.

Based on the dimension difference in Table 1, the accuracy of the dimension of the reconstructed 3D model has been calculated using equation 1. Fig. 4 shows the comparison of dimension accuracy between mobile photogrammetry and high-end scanner for test piece X, Y, G, and H. In overall, both 3D scanning approaches have a very high dimensional accuracy with an overall average of 97.18% and 97.83% for mobile photogrammetry and high-end scanner, respectively. The maximum and minimum accuracy by mobile photogrammetry is 99.9% at *g2* and 83.33% at *h1*, respectively. On the other hand, for the high-end 3D scanner, the maximum and minimum accuracy are 100% at *y2* and 84.01% at *h1*. Both approaches obtained the least accuracy at *h1* since there was a small slope of approximately 3^{o} at the surface of *h1*. Such results indicate that such undetectable small slope is the limit of these 3D scanning methods. Furthermore, for a geometry of 150 mm in size or above, it is found that photogrammetry method could achieve an accuracy above 98%, whereas the accuracy of small size geometry less than 10 mm, it could drop to 83%. Such findings demonstrated that the larger the object size, the accurate the 3D reconstruction of the model. Thus, in order to get the highest accuracy for the photogrammetry method, it is recommended to scan test pieces with a larger geometrical dimension, preferably more than 150 mm.

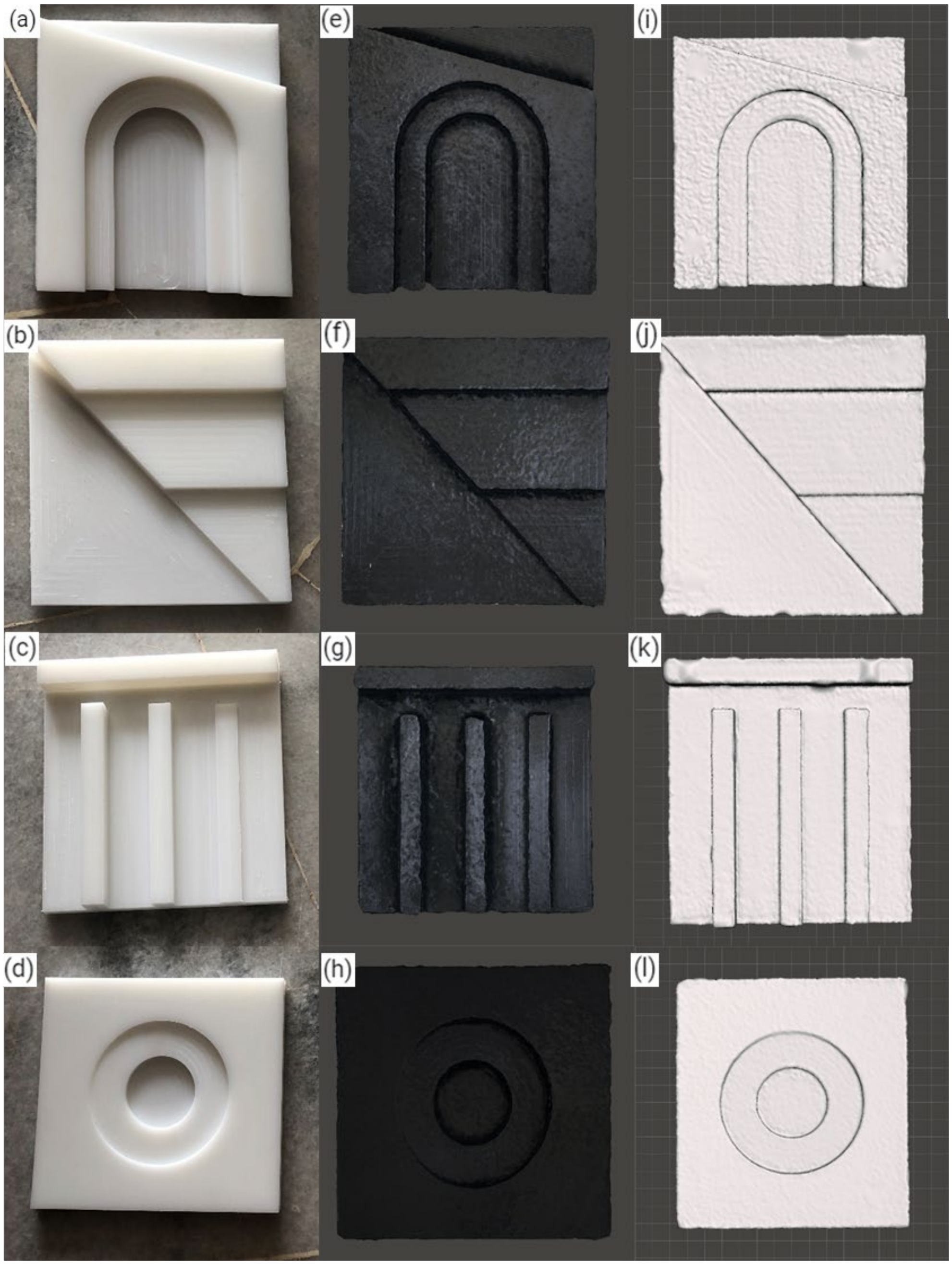

Fig. 3 - Comparison among fabricated test pieces, reconstructed 3D models by low and high-cost 3D scanning system (a)~(d) original test pieces *X*, *Y*, *G* and *H*, respectively; (e)~(h) reconstructed 3D models using photogrammetry technique by Meshroom software, and; (i)~(l) reconstructed 3D models using high-end 3D scanner by VXelements software

Table 1 - Dimensional accuracy of 3D scanning approaches

Test Piece	Label	Unit	Designed Dim.	Fabricated Dim.	Mobile Photogrammetry		High-end 3D Scanner	
					Reconstructed Dimension	Diff.	Reconstructed Dimension	Diff.
X	*x1*	mm	30	30.07	29.69	-0.38	30.30	0.23
	x2	°	100	100.21	100.88	0.67	100.33	0.13
	x3	°	60	55.23	61.09	5.86	60.23	5.00
	x4	mm	43.14	43.18	44.53	1.36	43.32	0.15
	x5	mm	30.5	30.51	31.14	0.63	30.03	-0.48
	x6	mm	50.5	50.49	50.84	0.35	50.67	0.18
	x7	mm	110.5	110.50	111.60	1.11	110.53	0.04
	x8	mm	130.5	130.50	130.94	0.44	130.39	-0.10
	x9	mm	161	161.03	162.43	1.40	161.39	0.36
	x10	mm	87.5	87.56	88.84	1.28	87.26	-0.30
	x11	mm	175	175.02	176.94	1.92	175.09	0.07
	x12	mm	5	5.77	5.32	-0.45	5.55	-0.22
	x13	mm	20	20.31	20.89	0.58	20.08	-0.23
	x14	mm	8	8.06	7.53	-0.53	7.66	-0.41
	x15	mm	7	7.58	7.02	-0.56	7.29	-0.29
	x16	mm	10	10.06	10.37	0.32	9.36	-0.70
Y	*y1*	°	45	45.04	45.72	0.68	45.45	0.41
	y2	mm	175	175.05	175.35	0.30	175.04	0.00
	y3	mm	31	31.11	31.75	0.64	31.73	0.62
	y4	mm	91	91.13	91.50	0.37	91.46	0.33
	y5	mm	161	161.03	161.65	0.62	161.12	0.09
	y6	mm	8	8.41	8.22	-0.19	8.29	-0.12
	y7	mm	13	13.45	13.58	0.13	13.49	0.04
	y8	mm	20	20.36	20.71	0.35	20.55	0.19
	y9	mm	5	5.01	4.92	-0.09	4.92	-0.09
G	*g1*	mm	131	130.81	131.35	0.54	131.06	0.26
	g2	mm	146	146.22	146.35	0.14	145.01	-1.20
	g3	mm	161	161.09	160.10	-0.99	160.22	-0.86
	g4	mm	30	30.08	28.41	-1.68	28.62	-1.46
	g5	mm	45	45.24	44.44	-0.80	44.58	-0.66
	g6	mm	75	75.50	76.49	0.99	76.58	1.08
	g7	mm	90	90.15	91.61	1.46	91.49	1.34
	g8	mm	120	120.05	119.46	-0.59	119.21	-0.84
	g9	mm	135	130.92	135.95	5.03	135.86	4.94
	g10	mm	165	165.02	166.56	1.54	165.01	-0.01
	g11	mm	7	7.38	7.81	0.43	7.61	0.23
	g12	mm	20	20.30	21.59	1.29	21.38	1.08
	g13	mm	15	15.30	14.76	-0.54	14.94	-0.36
	g14	mm	10	10.28	10.95	0.67	10.48	0.20
	g15	mm	20	20.29	19.36	-0.92	19.92	-0.37
H	*h1*	mm	10.83	9.28	10.83	1.55	10.76	1.48
	h2	mm	6	6.12	5.84	-0.29	6.67	0.55
	h3	mm	12	12.13	12.42	0.29	12.58	0.45
	h4	mm	20	20.00	19.80	-0.19	19.51	-0.48
	h5	°	100	100.01	98.73	-1.27	100.45	0.44
	h6	°	50	50.02	49.05	-0.97	50.38	0.36
	h7	mm	161	161.24	160.54	-0.70	160.85	-0.40
	h8	mm	175	175.06	172.27	-2.79	175.34	0.29

Additionally, the mean absolute error (MAE) and root-mean-square error (RMSE) were determined by the following equations:

$$MAE = \frac{1}{n}\sum_{j=1}^{n}\left|V_{observed,j} - V_{true,j}\right| \tag{2}$$

$$RMSE = \sqrt{\frac{1}{n}\sum_{j=1}^{n}\left(V_{observed,j} - V_{true,j}\right)^2} \tag{3}$$

Both MAE and RSME measure the average magnitude of the error of the 3D scanning method, without considering the positivity of the error itself. A smaller value indicates a higher accuracy of the method. MAE is useful in describing the deviation of observed values from the true ones. Meanwhile, for RMSE, since the measurement differences were squared before averaged, a larger error will become more significant and more useful in anticipating small differences in error values. The MAE and RSME for all test pieces obtained from both scanning methods are given in Figure 5. In overall, it can be observed that the high-end 3D scanner outperformed the mobile photogrammetry with MAE not more than 2.11%, except for test piece H where the MAE value is the largest (4.08%), even larger than that of mobile photogrammetry. A similar trend is also observed in RSME values for all test pieces. However, for test piece H, the RSME values of both methods only differ by 0.5%, which indicates a similarity in term of their performance. Test piece H contained extruded cut angular surfaces at all angles more than the other test pieces, which induced overshadowed areas that resulted in uncaptured blind spots [22]. Typically, both scanning methods had difficulty generating mesh for smaller size geometries of 10 mm or less, and thus, led to a slightly lower degree of accuracy. Even so, it was found that the largest differences in MAE and RSME values between both methods were 1.08% and 1.15%, respectively. Such a small difference indicates that there is no significant distinction between both methods.

Furthermore, two-way ANOVA analysis was also conducted to confirm that there is no significant difference in the accuracy of mobile photogrammetry and high-end scanner. Such fact was supported by the p-value in Table 2. The obtained p-value was 0.1758. A p-value larger than 0.05 indicates that the null hypothesis failed to be rejected. Thus, the ANOVA analysis confirmed that there was no significant accuracy difference between either scanning methods.

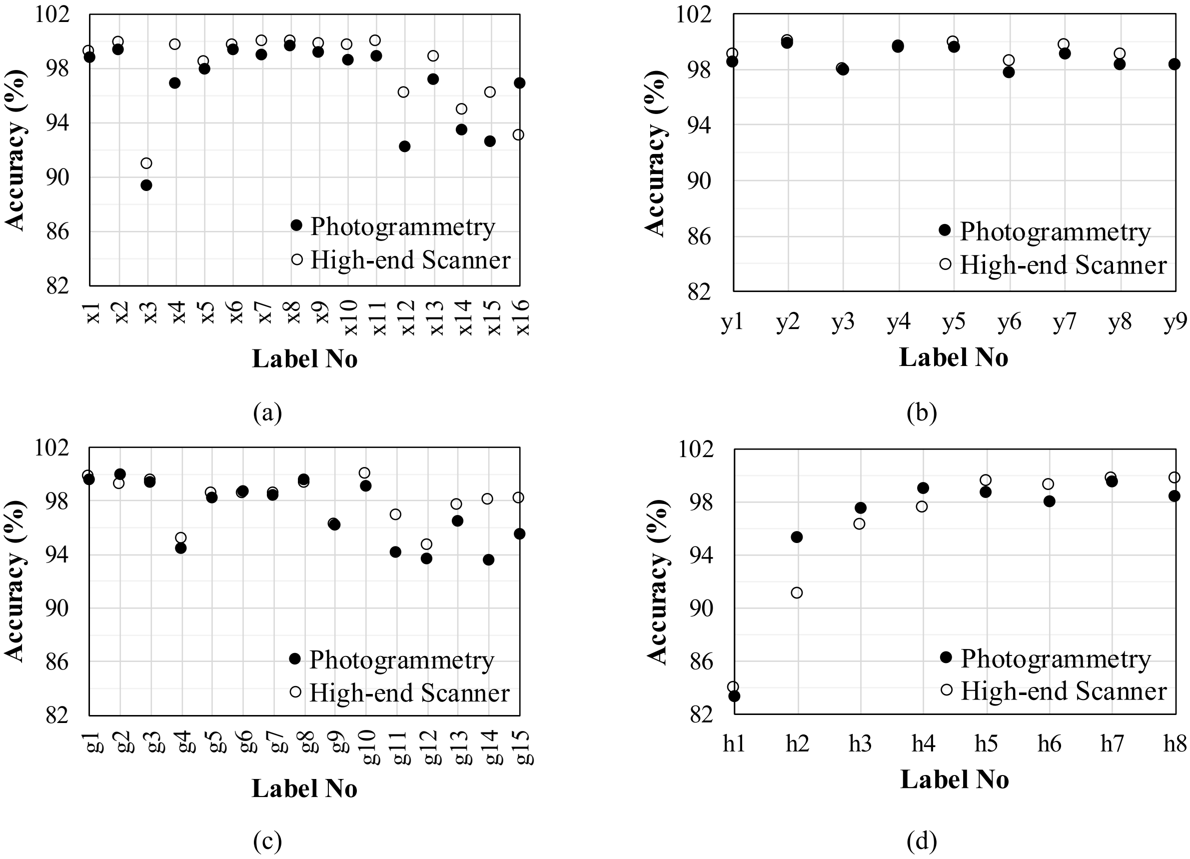

Fig. 4 - Comparison of dimension accuracy between mobile photogrammetry and high-end scanner for test piece (a) *X*; (b) *Y*;(c) *G*, and; (d) *H*

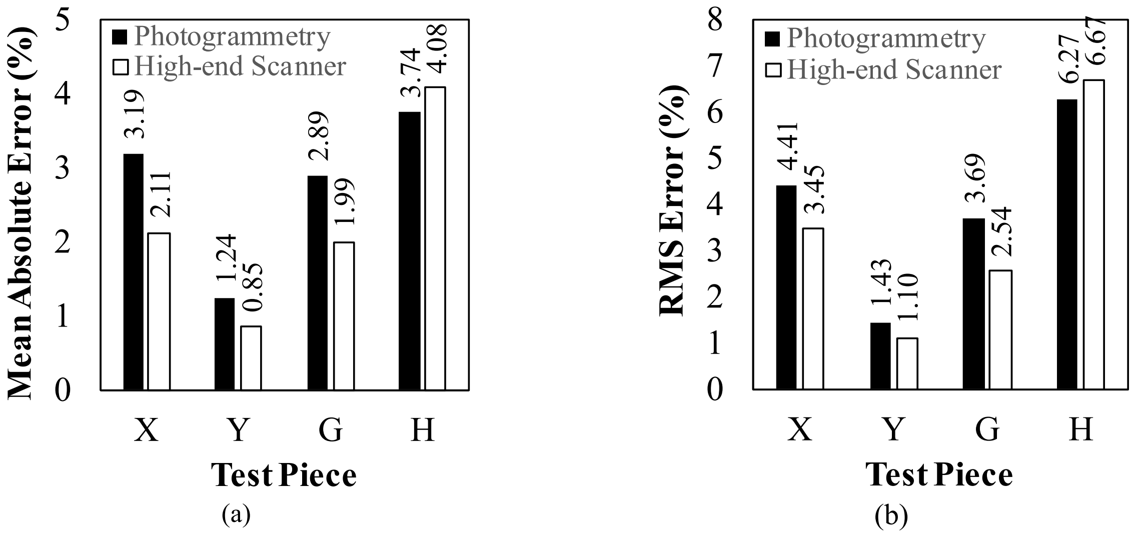

Fig. 5 - Comparison of (a) mean absolute error (MAE) and; (b) root-mean-square error (RMSE) between mobile photogrammetry and high-end scanner

Table 2 - ANOVA analysis between mobile photogrammetry and high-end scanner

Source of Variation	*SS*	*df*	*MS*	*F*	*p-value*	*F crit*
Label	339331.8	47	7219.826	20114.33	5.993×10^{-89}	1.623755
Scanning Method	0.678191	1	0.678191	1.88943	0.17578496	4.0471
Error	16.87016	47	0.35894			
Total	339349.4	95				

The data presented here makes it apparent that the photogrammetry 3D scan technique can be a useful tool for scanning sharp geometrical parts. Although the technique produces a model that less accurate than the high-cost 3D scan, but it is not significant. The photogrammetry was able to quickly capture the morphology of parts and produce a digital 3D model that requires only minimal post-processing. One particular advantage of using the photogrammetry method is the excellent quality of the mesh's surface, even though the resolution of photogrammetry is inferior than that of high-end scanner.

Despite the performance of the makeshift photogrammetry 3D scanning as discussed above, a few limitations on such techniques should be considered, especially since the current study investigated focused on simple solid geometries. Firstly, the accuracy of photogrammetry-based 3D scanning can be affected by the complexity of the object being scanned, particularly if it has irregular shapes or deep grooves that are difficult to capture with a mobile phone camera. For example, a study found that photogrammetry struggled to accurately capture the complex geometry of a human ear [23]. Thus, high-end 3D scanner should be opted for such cases. Secondly, such photogrammetry relies on capturing the external surface of an object to reconstruct its 3D model. Therefore, it may not be suitable for capturing the internal lattice structures of objects, such as those found in 3D-printed parts [24]. In a case where internal lattice structure is required, X-ray computed tomography (CT) could be used. Lastly, the proposed photogrammetry technique may struggle to accurately capture solid objects with opaque or reflective surfaces, as these can cause shadows or distortions in the images. In such cases, laser scanning is a better option [25].

4. Conclusion

The Photogrammetry method using a mobile phone has the potential to be utilized as a 3D scanner to capture images and obtain data for 3D model reconstruction having a sufficient resolution. In this study, for geometrical objects with dimensions from 5 to 175 mm, mobile photogrammetry achieved an average accuracy of 97.2%, with minimum and maximum values of 83.3% and 99.9%, respectively. In comparison with an industrial-grade high-end 3D scanner, two-way ANOVA analysis results with a p-value of 0.1758 provided a piece of evidence that there was no significant accuracy difference between both methods. Furthermore, it has been found that mobile photogrammetry surpassed the performance of the high-end scanner with a smaller value of RMSE (6.27%) for geometrical objects with a lot of curved surfaces. It is also found that a small tilting angle (less than 3°) is the scanning limit of either scanning methods. With such a makeshift 3D scanning by photogrammetry method using commonly available tools (mobile phone), it could rapidly advance the reverse engineering technology not only by major global industry players, but also private personal philanthropies for the benefit of society.

To further enhance the feasibility and accuracy of the makeshift 3D scanning system, there are several interesting avenues for future research. Firstly, it would be valuable to investigate the impact of different lighting conditions on the performance of the system, in order to gain a better understanding of how it affects the accuracy of the reconstructed 3D models. Additionally, it would be beneficial to evaluate the system's performance in outdoor and harsh environments, as this can provide important insights into its practical applicability in real-world scenarios. These future investigations can help to expand the scope of the research and contribute to the development of a more robust and versatile makeshift 3D scanning system.

Acknowledgement

The authors extend their sincere appreciation to the editor and reviewers for their time and valuable suggestions. The authors also gratefully acknowledge the facilities and financial support from Universiti Kuala Lumpur under Short Term Research Grants (str19015).

References

[1] Wozniak, A., Krajewski, G., & Byszewski, M. (2019). A new method for examining the dynamic performance of coordinate measuring machines. Measurement, 134, 814-819. doi: 10.1016/j.measurement.2018.12.041

[2] Piperi, E., Galantucci, L., Kaçani, J., Bodi, I., & Spahiu, T. (2017). 3D Low-cost scanning systems development for mechanical parts digi-talization. 1st International Conference Engineering and Entrepreneurship.

[3] Haleem, A., & Javaid, M. (2019). 3D scanning applications in medical field: A literature-based review. Clinical Epidemiology and Global Health, 7(2), 199-210. doi: 10.1016/j.cegh.2018.05.006

[4] Kersten, T. P., Lindstaedt, M., & Starosta, D. (2018). Comparative Geometrical Accuracy Investigations of Hand-Held 3D Scanning Systems; An Update. ISPRS - International Archives of the Photogrammetry, Remote Sensing and Spatial Information Sciences, XLII-2, 487-494. doi: 10.5194/isprs-archives-XLII-2-487-2018

[5] Boboc, R. G., Gîrbacia, F., Postelnicu, C. C., & Gîrbacia, T. (2019). Evaluation of Using Mobile Devices for 3D Reconstruction of Cultural Heritage Artifacts. VR Technologies in Cultural Heritage, VR Technologies in Cultural Heritage (VRTCH 2018), Brasov, Romania, May 29–30, 46-59.

[6] Lopez-Hawa, H., VanPelt, A., Emmanuel, S., & Yihun, Y. (2019). Automated Scanning Techniques Using UR5. Journal of Robotics 2019, 1-8. doi: 10.1155/2019/5304267

[7] Garcia, A. R., Miller, L. R., Andres, C. F., & Lorente, P. J. N. (2018). Obstacle Detection using a Time of Flight Range Camera. Paper presented at the 2018 IEEE International Conference on Vehicular Electronics and Safety (ICVES).

[8] Tran, V. L., & Lin, H.-Y. (2018). A Structured Light RGB-D Camera System for Accurate Depth Measurement. International Journal of Optics 2018, 1-7. doi: 10.1155/2018/8659847

[9] Falkingham, P. L. (2013). Low cost 3D scanning using off-the-shelf video gaming peripherals. Journal of Paleontological Techniques, 11, 1-9.

[10] Diakité, A. A., & Zlatanova, S. (2016). First Experiments with the Tango Tablet for Indoor Scanning. ISPRS Annals of Photogrammetry, Remote Sensing and Spatial Information Sciences, III-4, 67-72. doi: 10.5194/isprsannals-III-4-67-2016

[11] Galantucci, L. M., Piperi, E., Lavecchia, F., & Zhavo, A. (2015). Semi-automatic Low Cost 3D Laser Scanning Systems for Reverse Engineering. Procedia CIRP, 28, 94-99. doi: 10.1016/j.procir.2015.04.016

[12] Wang, Z. (2020). Review of real-time three-dimensional shape measurement techniques. Measurement, 156. doi: 10.1016/j.measurement.2020.107624

[13] Kenarsari, A. E., Vitton, S. J., & Beard, J. E. (2017). Creating 3D models of tractor tire footprints using close-range digital photogrammetry. Journal of Terramechanics, 74, 1-11. doi: 10.1016/j.jterra.2017.06.001

[14] Hassan, A. T., & Fritsch, D. (2019). Integration of Laser Scanning and Photogrammetry in 3D/4D Cultural Heritage Preservation–A Review. International Journal of Applied, 9(4).

[15] Alshawabkeh, Y., El-Khalili, M., Almasri, E., Bala'awi, F., & Al-Massarweh, A. (2020). Heritage documentation using laser scanner and photogrammetry. The case study of Qasr Al-Abidit, Jordan. Digital Applications in Archaeology and Cultural Heritage, 16. doi: 10.1016/j.daach.2019.e00133

[16] Donato, L., Cecchi, R., Goldoni, M., & Ubelaker, D. H. (2020). Photogrammetry vs CT Scan: Evaluation of Accuracy of a Low-Cost Three-Dimensional Acquisition Method for Forensic Facial Approximation. Journal of Forensic Sciences. doi: 10.1111/1556-4029.14319

[17] Casella, E., Drechsel, J., Winter, C., Benninghoff, M., & Rovere, A. (2020). Accuracy of sand beach topography surveying by drones and photogrammetry. Geo-Marine Letters, 40(2), 255-268. doi: 10.1007/s00367-020-00638-8

[18] Jang, H., Kitahara, I., Kawamura, Y., Endo, Y., Topal, E., Degawa, R., & Mazara, S. (2019). Development of 3D rock fragmentation measurement system using photogrammetry. International Journal of Mining, Reclamation and Environment, 34(4), 294-305. doi: 10.1080/17480930.2019.1585597

[19] Bogdan, S. L., Nedelcu, D., & Pădurean, I. (2019). The Reverse Engineering technique performed on a Francis Runner Geometry through Photogrammetry. IOP Conference Series: Materials Science and Engineering, 477. doi: 10.1088/1757-899x/477/1/012021

[20] Nedelcu, D., Gillich, G. R., Gerocs, A., & Padurean, I. (2020). A comparative study between photogrammetry and laser technology applied on model turbine blades. Journal of Physics: Conference Series, 1426. doi: 10.1088/1742-6596/1426/1/012026

[21] Donlic, M., Petkovic, T., & Pribanic, T. (2017). On tablet 3D structured light reconstruction and registration. Paper presented at the Proceedings of the IEEE International Conference on Computer Vision Workshops.

[22] Kwon, S., Park, J.-W., Moon, D., Jung, S., & Park, H. (2017). Smart Merging Method for Hybrid Point Cloud Data using UAV and LIDAR in Earthwork Construction. Procedia Engineering, 196, 21-28. doi: 10.1016/j.proeng.2017.07.168

[23] El-Sheimy, N., Abdel-Rahman, M., & Farid, A. (2018). Photogrammetry-based 3D modeling of the human ear: Accuracy assessment. Measurement, 124, 38-47.

[24] Saniman, M. N. F., Hashim, M. M., Mohammad, K. A., Abd Wahid, K. A., Muhamad, W. W., & Mohamed, N. N. (2020). Tensile characteristics of low density infill patterns for mass reduction of 3D printed polylactic parts. International Journal of Automotive and Mechanical Engineering, 17(2), 7927-7934.

[25] Júnior, A. M. A., Vieira, M. A., Silva, V. D., & Gonçalves, D. C. (2019). Comparison of photogrammetry and laser scanning for 3D modeling of a reflective surface. Journal of Applied Geodesy, 13(1), 1-11.